

# CRLH LWA Using Mushroom-Like Structures for Improved Radiation Performances

Huan Zhang\*

**Abstract**—A composite right/left-handed (CRLH) leaky wave antenna (LWA) using double mushroom-like structures is proposed. With a proper arrangement of the left-handed structures, desirable cross-polarization performance in two orthogonal planes can be obtained based on the differential excitation principle. The CRLH performance of the cascaded LWA is demonstrated, and the improved radiation performance is clarified. Measured results indicate that the proposed antenna operates in 9.7–16.4 GHz with a beam scanning range from  $-71^\circ$  to  $+31^\circ$ . The cross-polarization levels are less than  $-30$  dB and  $-20$  dB in the beam scanning plane and non-beam-scanning plane, respectively.

## 1. INTRODUCTION

In recent years, leaky wave antennas (LWAs) have received much attention in radar and multipoint communication fields for their frequency-scanning capabilities [1]. Considerable attention has been paid to the composite right/left-handed (CRLH) LWAs in the past few years [2–8]. With CRLH structures, negative phase velocity is acquired, and backward radiation appears due to the negative wavenumber. In [2], four types of LWAs with interdigital slots as series capacitors were implemented and analysed. Continuous beam-scanning feature was achieved. A composite CRLH LWA with wide-angle scanning range was designed with beam scanning range from  $-56^\circ$  to  $+51^\circ$  in frequency band 5.1–6.11 GHz [3]. In [4], a compact CRLH LWA using a TE<sub>20</sub> mode substrate integrated waveguide (SIW) was proposed, and the balanced LWA can scan its main beam from  $-75^\circ$  to  $+49^\circ$  with a peak gain of 18 dBi. Double periodic CRLH-SIW was also used in LWA design [5]. With this arrangement, a new leaky region can be observed in addition to the regular CRLH characteristic. To achieve larger scanning angle, composite phase-shifting transmission lines were utilized in [6] to realize larger phase slopes. A novel metamaterial-based LWA was designed to improve its radiation bandwidth in the boresight direction [7]. Besides, a CRLH-based half mode substrate integrated waveguide (HMSIW) can also be used in circularly polarized (CP) LWA designs. In [8], a CRLH-HMSIW-based CP LWA with backward-broadside-forward radiation was presented.

In this paper, a balanced CRLH-SIW-based LWA is proposed. Firstly, unit cell analyses are done to demonstrate its CRLH feature, and the electric field distributions are studied to show the radiation feature. Then, investigations on the cascaded LWA are done based on the unit cell analyses. The proposed LWA operates in 9.7–16.4 GHz (51.3% centred at 13.05 GHz) with a beam scanning range from  $-71^\circ$  to  $+31^\circ$ , and its cross-polarization levels in the beam scanning plane are less than  $-30$  dB. Compared with our previous design in [9], improved radiator arrangement is adopted here for better radiation performance in the non-beam-scanning plane, which is discussed in the following sections.

---

*Received 30 December 2020, Accepted 5 February 2021, Scheduled 18 February 2021*

\* Corresponding author: Huan Zhang (zhmfpp@163.com).

The author is with the Xi'an Research Institute of Navigation Technology, Xi'an, Shaanxi 710068, China.

## 2. DESIGN OF CRLH-SIW BASED LWA

The proposed unit-cell structure is shown in Figure 1. It consists of three layers: top layer, bottom layer, and substrate layer made of inexpensive FR4 with relative permittivity  $\epsilon_r = 4.4$  and thickness  $h = 1$  mm. Two columns of mushroom-like radiators are placed symmetrically with respect to the longitude centre line. The parameter values are:  $s = 13.1$  mm,  $p = 11$  mm,  $h = 1$  mm,  $d1 = 4.8$  mm,  $d2 = 4.2$  mm,  $d3 = 1$  mm,  $d4 = 0.7$  mm,  $Di = 0.8$  mm,  $W1 = 2.6$  mm,  $W2 = 1.6$  mm.

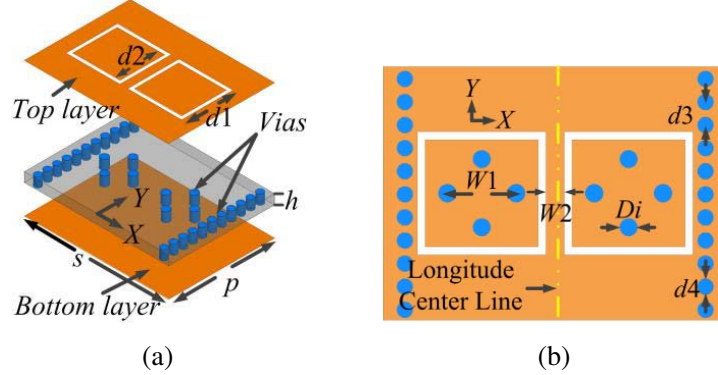


**Figure 1.** Structure of the proposed unit cell. (a) 3-D view, and (b) top view.

### 2.1. Unit Cell Analysis

The extracted initial equivalent circuit of the proposed unit cell is presented in Figure 2(a). Two mushroom-like structures are modelled as a shunt resonator tank characterized by the right-handed capacitor  $C_{R2}$  and left-handed inductor  $L_{L2}$ . Left-handed capacitors  $C_L$  are related to the square slot rings in broad face of the SIW structure. Other extracted components in Figure 2(a) are naturally related to the SIW structure [2]. Two left-handed (LH) units are introduced in parallel to guarantee the CRLH performance, and the slot rings act as radiators from which energy leaks out. Considering symmetry of the structure, the circuit in Figure 2(a) is simplified to the one in Figure 2(b). Values of the extracted lumped components in Figure 2(b) can be acquired by the AWR software with the data fitting method [10]. The extracted values are:  $L_{L1} = 1.35$  nH,  $L_{L2} = 0.14$  nH,  $L_{R1} = 0.703$  nH,  $L_{R2} = 3.3$  nH,  $C_L = 0.29$  pF,  $C_{R1} = 0.16$  pF, and  $C_{R2} = 0.87$  pF.

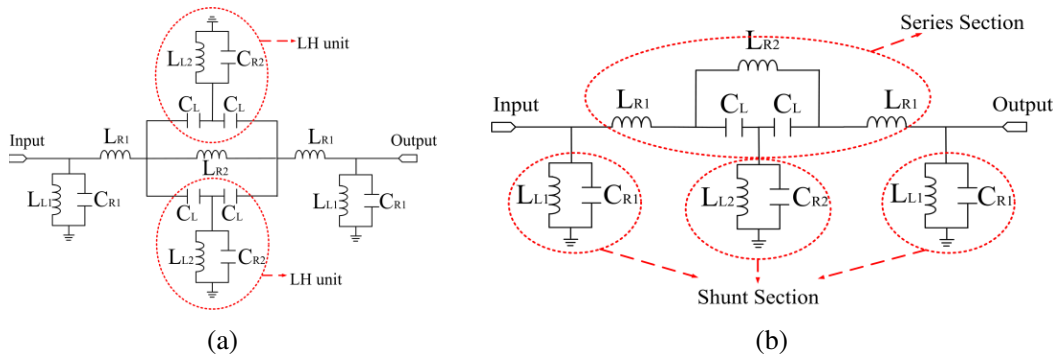


**Figure 2.** Extracted losses equivalent circuit of the proposed unit cell. (a) Initial version, and (b) simplified version.

Unit cell parameters obtained from the full-wave simulation and the circuit model are presented in Figure 3, and their good agreements validate the equivalent circuit. For the simplified circuit, its series resonance frequency  $\omega_{se}$  is 13.32 GHz, and its shunt resonance frequency  $\omega_{sh}$  is 13.47 GHz, which means

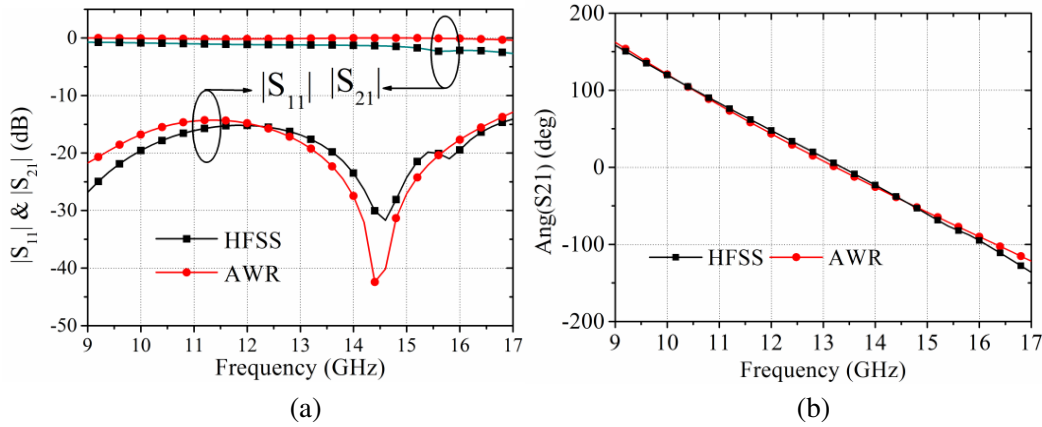


Figure 3.  $S$ -parameters of the proposed unit cell. (a) Magnitude, and (b) phase.

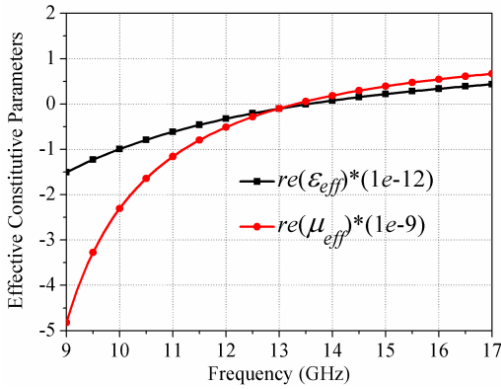


Figure 4. Extracted effective constitutive parameters for the proposed unit cell.

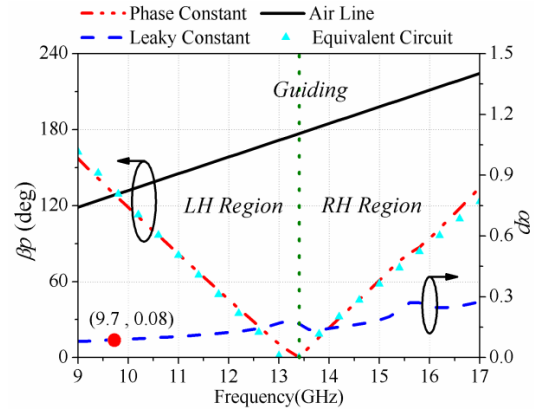
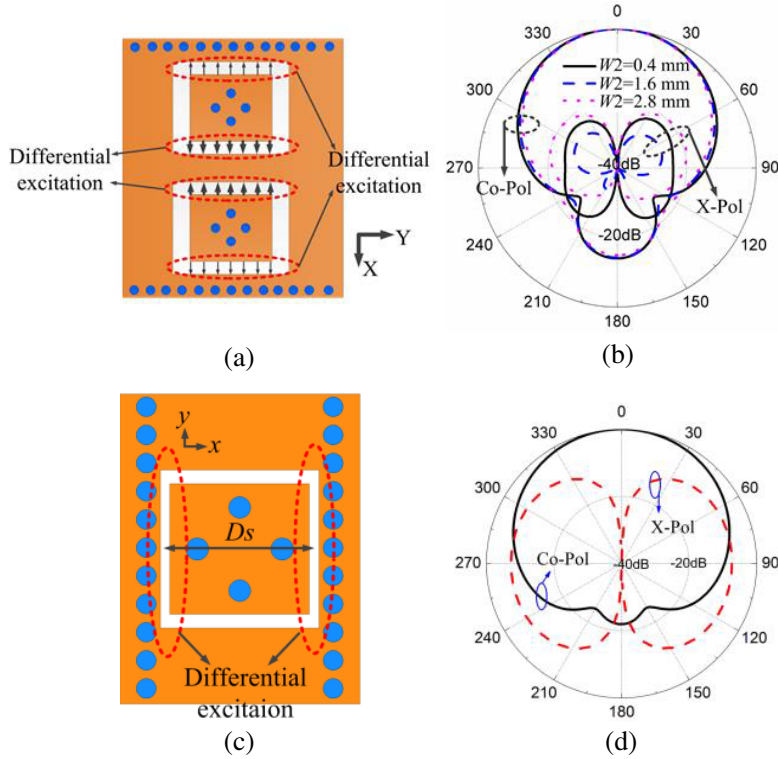


Figure 5. Dispersion feature of the proposed unit cell.

that the balanced condition  $\omega_{se} = \omega_{sh}$  is approximately satisfied. The extracted effective constitutive parameters [10] for the proposed unit cell are given in Figure 4. Double negative performance in the LH region is clearly observed, and the transition frequency is around 13.4 GHz as shown in the figure. Unit cell dispersion properties are plotted in Figure 5. The radiation region starts from about 9.7 GHz, and the transition point occurs at 13.4 GHz. The phase constant derived from the equivalent circuit with  $S$ -parameter method [11] is also given in Figure 5. Acceptable agreement further validates the circuit.

Far field radiations of the unit cell are discussed. As shown in Figure 6(a), four  $y$ -oriented slots can be divided into two groups, and each group has two differentially excited radiating slots. Considering far field radiation in the beam scanning plane (i.e.,  $yo$ z plane), the cross-polarization (Phi-polarization) levels are expected to be low according to the superposition principle of the electromagnetic field. Unit-cell radiation patterns in  $xoz$  plane at the transition frequency with different  $W2$  values are given in Figure 6(b). The cross-polarization (Theta-polarization) is mainly produced by two  $y$ -oriented slots near the longitude centre line, where the electric field distribution is much stronger than that near the via walls. Due to small  $W2$  value, low cross-polarization levels will be expected in  $xoz$  plane. However, the cross-polarization levels may become worse as  $W2$  value decreases, because the effect of two slots near the SIW via walls cannot be neglected any more in this case. Compared with the unit cell in our previous work [9], whose radiation mechanism in  $xoz$  plane is shown in Figure 6(c), the proposed unit cell herein has an improvement of lower cross-polarization levels in  $xoz$  plane. This is because less phase difference is introduced between two differentially excited slots for the proposed design as  $W2 < D_s$ . Effects of some critical parameters on the phase constant  $\beta$  and the leaky constant  $\alpha$  are also analysed.

Figure 7(a) indicates that the unit cell periodicity  $p$  has a great influence on the phase constant. Larger periodicity leads to lower transition frequency point. The leakage per unit cell can be controlled by changing dimensions of the slot rings from which the energy leaks out, as shown in Figure 7(b).



**Figure 6.** Clarification of the unit cell radiation. (a) Differential excitation of the proposed design, (b) radiation patterns in  $xoz$  plane of the proposed design, (c) differential excitation of the design in our previous work, (d) radiation patterns in  $xoz$  plane of the design in our previous work.

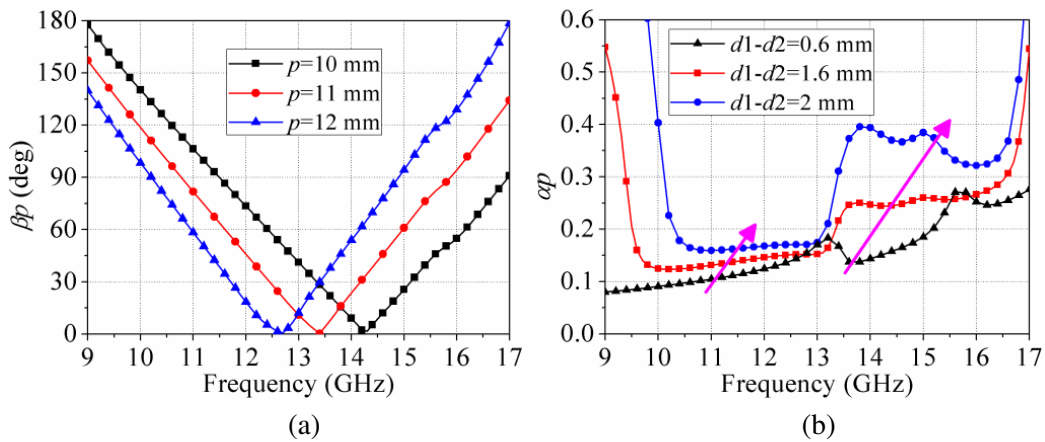


**Figure 7.** Parametric analyses for the proposed unit cell. (a) Phase constants with different  $p$  values, (b) leaky constants with different  $(d1-d2)$  values.

### 2.2. Cascaded LWA Performances

The proposed SIW-based LWA is constructed by cascading its unit cells in series. The simulated gain curve is shown in Figure 8. Obviously, 12 unit cells are enough for the power leakage. The proposed LWA

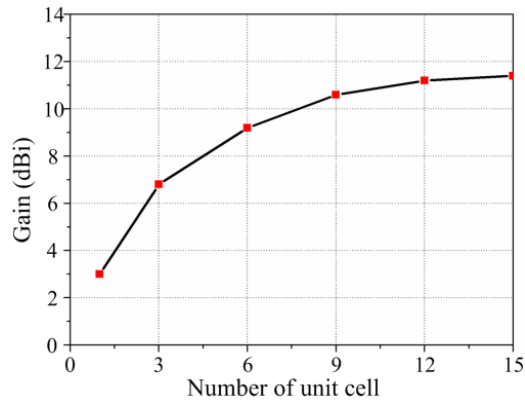


Figure 8. Gain versus number of the unit cell at the transition frequency.

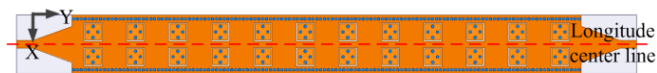


Figure 9. Structure of the SIW-based LWA with 12 units.

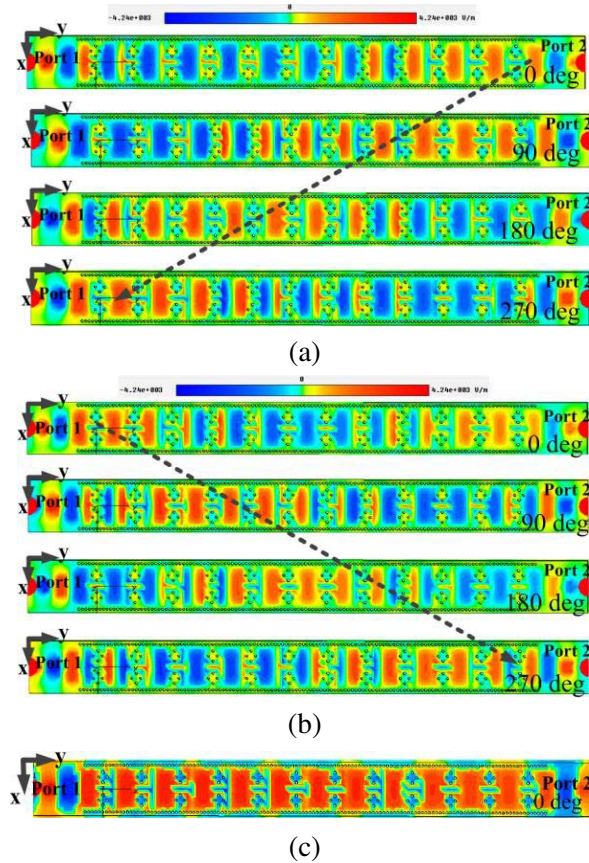
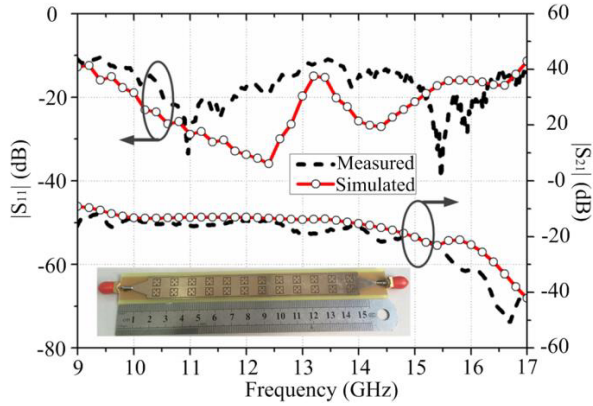


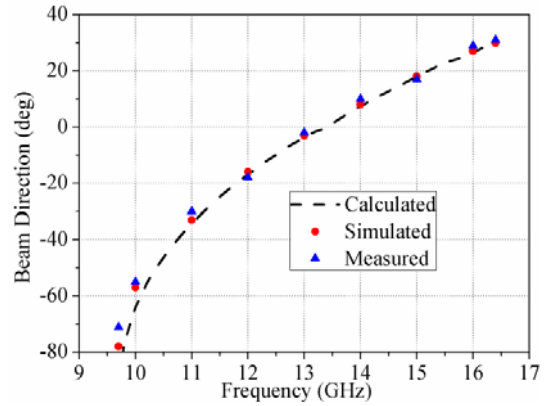
Figure 10. Electric field distribution in  $+z$  direction at different frequencies. (a) 12.5 GHz, (b) 14 GHz and (c) 13.4 GHz.



structure is given in Figure 9, and the simulated electric fields in  $+z$  direction at different frequencies are presented in Figure 10. The left-handed transmission feature is clearly observed, and infinite guided wavelength is obtained at the transition frequency. The antenna is fabricated and measured with  $S$ -parameters given in Figure 11. For both the simulated and measured results, the impedance band ranges from about 9 GHz to more than 17 GHz, and  $|S_{21}|$  values are lower than  $-10$  dB across the operating frequency band, indicating that 12 unit cells are sufficient for the energy leakage. The main beam directions calculated by  $\theta = \sin^{-1}(\beta(\omega)/k_0)$  are plotted in Figure 12 to make the beam scanning feature clear. The main beam points to the broadside direction at the transition frequency and scans to backward or forward directions as the frequency decreases or increases. The simulated and measured beam directions are also given in the same figure. Good agreements are observed.



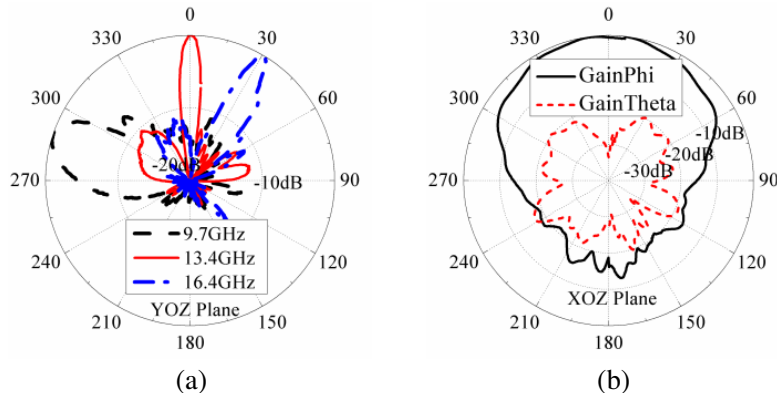
**Figure 11.**  $S$ -parameters of the SIW-based LWA.



**Figure 12.** Comparison of the main beam directions.

Measured radiation patterns in  $yoz$  plane at three different frequencies are shown in Figure 13(a). Continuous scanning ability is demonstrated. The main beam scans from  $-71^\circ$  to  $31^\circ$  as the frequency ranges from 9.7 GHz to 16.4 GHz, and the broadside radiation appears at 13.4 GHz.

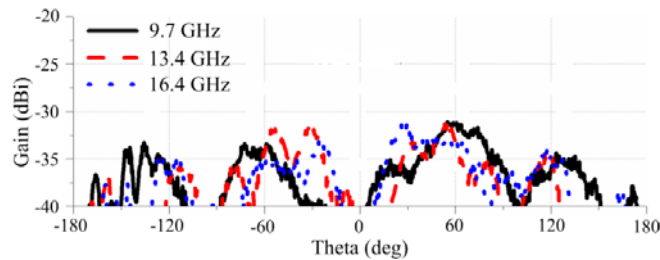
Moreover, measured radiation patterns in  $xoz$  plane at the balanced point are presented in Figure 13(b), and around  $-20$  dB cross-polarization levels are obtained. Cross-polarization feature in the beam scanning plane at different frequencies is plotted in Figure 14. Low XPLs (less than  $-30$  dB) are achieved due to the differential excitations of the  $y$ -oriented slots [12]. Measured antenna peak gains are above 9 dBi, and the gain variation is less than 1.6 dBi across the whole operating band. The proposed antenna is compared with some existing LWAs published previously, as shown in Table 1. Lower cross-polarization levels are obtained in the beam scanning plane for our design. This is mainly due to the differential excitations of the  $y$ -oriented radiating slots.



**Figure 13.** Measured radiation patterns. (a)  $yoz$  plane at different frequencies, and (b)  $xoz$  plane at the transition frequency.

**Table 1.** Comparison of the proposed antenna with some existing LWAs.

Reference	Antenna type	Beam scanning range	Normalized X-pol in beam scanning plane (dBi)	Operating band	Maximum gain (dBi)
[2] (Single-sided)	Single-layered	$-70^\circ$ – $+60^\circ$	$\approx -25$	8.6–12.8 GHz	12.8
[7]	Multi-layered	$-60^\circ$ – $+60^\circ$	$\approx -15$	8–13 GHz	14.8
[13] (X-polarized)	Single-layered	$-35^\circ$ – $+45^\circ$	$< -10$	7.5–10 GHz	11.75
[13] (Y-polarized)	Single-layered	$-30^\circ$ – $+45^\circ$	$< -10$	7.5–10 GHz	11.13
Our work	Single-layered	$-71^\circ$ – $+31^\circ$	$< -30$	9.7–16.4 GHz	10.6

**Figure 14.** Normalized cross-polarization levels in the beam scanning plane.

### 3. CONCLUSIONS

A novel CRLH-SIW-based leaky wave antenna with low cross-polarization levels is designed herein. Mushroom-like structures are utilized for the CRLH transmission feature, and the differential excitation principle is used for low cross polarization levels. Equivalent circuit of the proposed unit cell is extracted, and its CRLH performance is demonstrated. The cascaded LWA is verified to have wide beam scanning range (from  $-71^\circ$  to  $+31^\circ$ ) in 9.7–16.4 GHz band and low cross-polarization levels in both two orthogonal planes. The proposed LWA may be suitable for applications where continuous frequency-beam-scanning ability and low XPL features are preferred.

### REFERENCES

1. Singh, M. and B. Ghosh, "Periodic strip loaded reconfigurable half-mode substrate integrated waveguide-based leaky wave antennas," *Electron. Lett.*, Vol. 56, No. 13, 646–648, 2020.
2. Dong, Y. and T. Itoh, "Composite right/left-handed substrate integrated waveguide and half mode substrate integrated waveguide leaky-wave structures," *IEEE Trans. Antennas Propag.*, Vol. 59, No. 3, 767–775, March 2011.
3. Karmokar, D. K., Y. J. Guo, et al., "Composite right/left-handed leaky-wave antennas for wide-angle beam scanning with flexibly chosen frequency range," *IEEE Trans. Antennas Propag.*, Vol. 68, No. 1, 100–110, January 2020.
4. Sarkar, A., A. Sharma, et al., "Compact CRLH leaky wave antenna using TE<sub>20</sub>-mode substrate integrated waveguide for broad space radiation coverage," *IEEE Trans. Antennas Propag.*, Vol. 68, No. 10, 7202–7207, October 2020.

5. Jin, C. and A. Alphones, "Leaky-wave radiation behavior from a double periodic composite right/left-handed substrate integrated waveguide," *IEEE Trans. Antennas Propag.*, Vol. 60, No. 4, 1727–1735, April 2012.
6. Cao, W., Z. N. Chen, and W. Hong, "A beam scanning leaky-wave slot antenna with enhanced scanning angle range and flat gain characteristic using composite phase-shifting transmission line," *IEEE Trans. Antennas Propag.*, Vol. 62, No. 11, 5871–5875, November 2014.
7. Nasimuddin, N., Z. N. Chen, and W. Qing, "Substrate integrated metamaterial-based leaky-wave antenna with improved boresight radiation bandwidth," *IEEE Trans. Antennas Propag.*, Vol. 61, No. 7, 3451–3457, June 2013.
8. Saghati, A. P., M. M. Mirsalehi, and M. H. Neshatid, "A HMSIW circularly polarized leaky-wave antenna with backward, broadside, and forward radiation," *IEEE Antennas Wireless Propag. Lett.*, Vol. 13, 2320–2325, 2014.
9. Zhang, H., Y. C. Jiao, and G. Zhao, "CRLH-SIW-based leaky wave antenna with low cross-polarisation for Ku-band applications," *Electron. Lett.*, Vol. 52, No. 17, 1426–1428, 2016.
10. Caloz, T. I., *Electromagnetic Metamaterials: Transmission Line Theory and Microwave Applications*, Wiley, Hoboken, 2004.
11. *Left-handed Metamaterial Design Guide*, Ansoft Corporation, 2007.
12. Schejbal, V. and V. Kovarik, "A method of cross-polarization reduction," *IEEE Antennas Propag. Mag.*, Vol. 48, No. 5, 108–111, 2006.
13. Dong, Y. and T. Itoh, "Substrate integrated composite right-/left-handed leaky-wave structure for polarization-flexible antenna application," *IEEE Trans. Antennas Propag.*, Vol. 60, No. 2, 760–771, February 2012.